NEURON-INSPIRED COMPUTATIONAL E-SKIN WITH DEVICE-INTRINSIC IN-SENSOR COMPUTING AND SELF-POWERED COMPREHENSIVE TACTILE PERCEPTION

*Xinge Guo[1], Jingfeng Xu[1], Luwei Wang[1], and Chengkuo Lee[1]**

[1] Department of Electrical & Computer Engineering, National University of Singapore, Singapore

ABSTRACT

This work reports a neuron-inspired, self-powered electronic skin (E-Skin) that combines device-intrinsic in-sensor computing with tactile perception for large-area, low-power robotic touch. A soft PVA/PAAm/LiCl ionic hydrogel array converts mechanical stimuli into voltage signals, implements geometry-programmed, pixel-wise ionic conductance weights, and physically compresses 40 sensing pixels into two readout channels with zero external power and no active ICs. Despite a 95% reduction in channel count, the E-skin preserves salient per-pixel information: single-pixel fingertips distinguish hardness and roughness with 95.0% and 92.8% accuracy, resolve 20 visually similar materials with 98.83% accuracy beyond human performance, and reconstruct contact locations from compressed outputs with 95.33% accuracy. When deployed on a robotic hand, the two-channel, self-powered readout discriminates 29 everyday objects with 99.25% accuracy and demonstrates low-latency tactile inference. This architecture shifts computation into the sensor body, alleviates compute bottlenecks that limit large-area E-skins, and offers a generalizable route to ultra-low-power tactile interfaces for future human–robot interaction.

KEYWORDS

Tactile Sensor, In-Sensor Computing, Robot, E-Skin, Artificial Intelligence.

INTRODUCTION

Robots have rapidly evolved from a traditional automation tool into a core technology driving the next wave of industrial and societal transformation. Human expectations for robots have shifted from executing repetitive and straightforward tasks to acting as intelligent partners capable of facilitating and improving human–machine and even human-human interactions. Nowadays, robots are increasingly integrated into manufacturing, healthcare, service, education, and domestic environments, forming a critical infrastructure that enhances productivity, safety, and quality of life [1], [2], [3]. However, realizing advanced interaction requires robots to possess a comprehensive perception of the physical world [4], [5], [6]. The development of tactile sensing for robotic hands is of great significance for comprehensive perception in robots[7], [8]. For example, researchers utilize combinations of triboelectric, piezoelectric, piezoresistive, or capacitive mechanisms to achieve multimodal, comprehensive tactile perception [9], [10]. However, a single-pixel tactile sensing unit alone is difficult to achieve comprehensive tactile perception across the entire robotic skin [11], [12], [13]. To further expand the sensing area and obtain richer tactile information, researchers have developed large-area platforms, such as electronic gloves

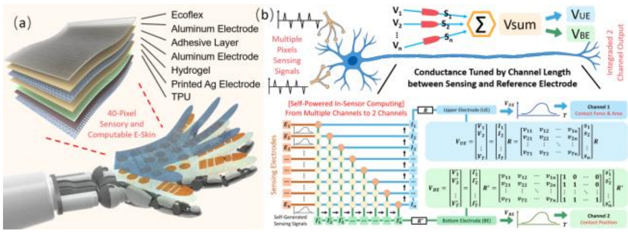

Figure 1: Neuron-Inspired Robotic E-Skin with Comprehensive Tactile Perception and In-Sensor Computing: (a) Illustration of the E-Skin; (b) Layers and Materials; (c) Detailed Principles

and intelligent insoles, equipped with multiple tactile sensor arrays [14], [15], [16], [17]. However, such a design with extensive output channels inevitably generates substantial data, requiring complex peripheral circuits and increasing the computational burden of reading and processing. It not only increases hardware complexity, energy consumption, latency, and data storage requirements, but also poses an essential obstacle to the integration of tactile sensors [18], [19], [20], [21]. For example, Yan et al. developed a flexible, self-powered frictional electric sensor array using laser-induced graphene, which is still affected by wiring complexity and crosstalk even at a large scale [22] .

Herein, a self-powered, neuron-inspired computational E-Skin that integrates comprehensive tactile perception with in-sensor computing is introduced. This system uniquely achieves geometry-defined channel compression while exhibiting human-augmented comprehensive tactile perception. Firstly, the device fabrication leverages a composite structure comprising printed Ag Electrodes embedded in a Thermoplastic Polyurethane (TPU) substrate, an aluminum electrode with an adhesive layer, Ecoflex, and hydrogel (**Fig. 1(a)**). It exhibits good flexibility and can tightly adhere to the palm (**Fig. 1(a)**). The single-pixel fingertip of the E-Skin can realize human-augmented perception. It can distinguish surface hardness and roughness with accuracies of 95.0% and 92.8%, respectively. It also successfully classifies 20 similar materials with 98.83% accuracy, which is significantly higher than human tactile perception capability. Based on this, the single pixel is expanded to a large-area palm E-skin with 40 sensing pixels. Inspired by neural convergence in the somatosensory pathway, multiple pixel-sensing signals serve as synapses in the E-Skin's electronic neural network. They are further consolidated into two integrated output channels via axons of varying lengths, forming the geometry-defined channel compression strategy (**Fig. 1(b)**). More importantly, this process preserves salient tactile features while enabling precise reconstruction of contact points. The computational E-Skin demonstrates robust recognition capabilities, accurately identifying 29 daily objects with 99.25%

2026 IEEE 39th International Conference on Micro Electro Mechanical Systems (MEMS) | 979-8-3315-7251-8/26/$31.00 ©2026 IEEE | DOI: 10.1109/MEMS64181.2026.11419487

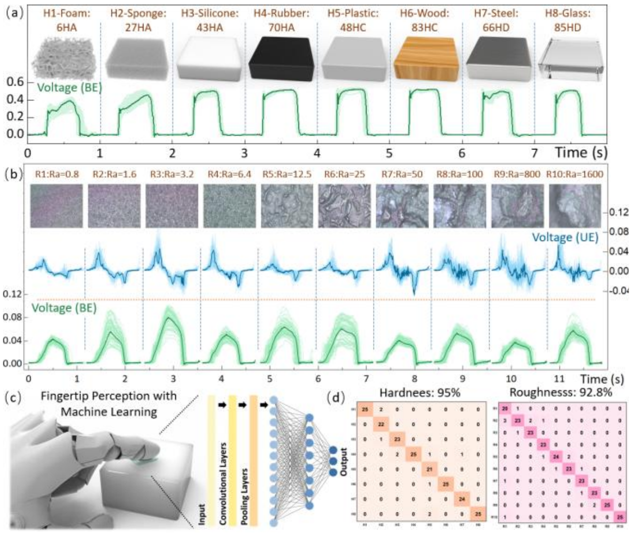

Figure 2: Tactile Perception of the E-Skin on the Fingertip. (a) Hardness ranging from extra soft to extra hard. (b) Surface roughness ranging from 0.8 μm to 1600 μm.(c) Illustration of fingertip contact and ML. (d) ML accuracy

accuracy with two unified channels. Furthermore, this principle can be generalized to implement flexible N-to-2 mappings for low-bandwidth, ultra-low-power tactile E-Skins in future robots, thereby providing an effective solution for comprehensive perception in next-generation intelligent robots.

PERFORMANCE CHARACTERIZATION

Sensing pixel endowed with human-augmented tactile perception capability

Hydrogels have been widely applied in multifunctional tactile sensors due to their good flexibility, high ductility, ionic conductivity, and a bionic three-dimensional network structure similar to biological tissues, which enables stable signal transmission. In this work, a hydrogel composed of polyvinyl alcohol (PVA), polyacrylamide (PAAm), lithium chloride (LiCl), and glycerol (Gly) ions has been developed as the intermediate medium. Fig. 2 illustrates the capability of single-pixel fingertip perception to distinguish various physical properties. To test the range of hardness perception, eight objects spanning from extra soft (6 HA) to extra hard (85 HD) are selected to test the hardness perception capability (**Fig. 2(a)**). When applying force to the objects, the instantaneous force feedback will rapidly increase the output voltage. The voltage output will show a rapid drop, then increase, as the object deforms. Due to the difference in Young's modulus, the soft object will deform more and provide less force feedback, leading to a higher growth rate in the voltage output. Regarding roughness perception, ten objects with varied roughness were selected. The range spans from 0.8 μm to 1600 μm which nearly covers the surface characteristics of everyday daily objects (**Fig. 2(b)**). The E-skin is tested through sliding from one end of these objects to the other without precisely controlling the scanning force. When sliding through, rough objects produce more frictional electrical signals due to a greater number of surface contact separations than smooth objects. Here, the fingertip contact mechanism is illustrated. The classification accuracies for hardness and roughness were

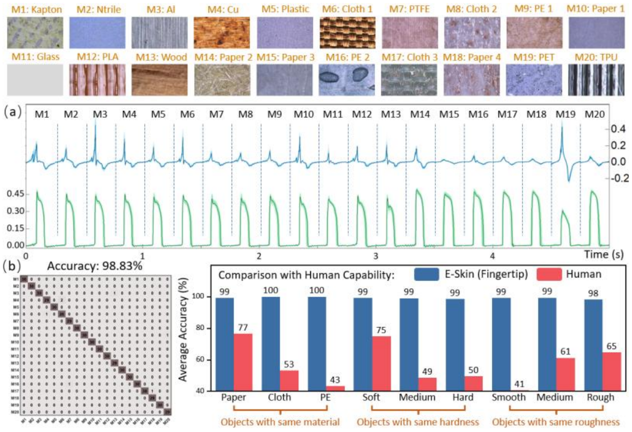

Figure 3: Human-Augmented Perception. (a) Discrimination of 20 different materials. (b) Comparison of accuracy with human tactile perception capability.

95.0% and 92.8%, respectively (Fig. 2(c, d)). Twenty different materials with similar roughness or hardness are selected to explore further its performance in identifying similar materials in daily life, with an accuracy of 98.83% (**Fig. 3(a, b)**). To demonstrate its human-augmented tactile perception capability, its performance is compared with the human perception result. For humans, material differentiation mainly relies on the spatial resolution ability of Merkel cell complexes. When the main characteristics (such as material, hardness, or roughness) of contact objects are similar, the signal patterns of multiple receptors tend to overlap, and the brain's integrated interpretation mechanism loses its distinct neural feature vector. A cohort of 20 human participants performs significantly worse with only 41-78% recognition accuracy compared to the E-Skin, underscoring its human-augmented perceptual resolution.

Device-Intrinsic In-Sensor Computing for Geometry-Defined Channel Compression

To achieve more comprehensive, large-scale object perception, more sensing units are required to detect multifaceted information. These sensor arrays require complex readout circuits and data storage, which significantly increases power consumption. Besides, a larger amount of data needs to be processed, which can also cause significant latency and privacy leakage issues. Inspired by neural convergence in the somatosensory pathway—where many synaptic inputs are integrated and relayed along a small number of axonal outputs, we try to imitate the neural structure to cut down the number of output channels. The conduct length of each sensing pixel is programmed to set pixel-wise ionic conductance weights, guiding the self-generated signals from a 40-pixel array into two channel-selective pathways toward a shared reference electrode for passive.

Firstly, based on the palm structure, the fingertip is expanded to the entire finger to verify the feasibility of device-intrinsic in-sensor computing. To assess the position recognition ability across different positions, 20 classes, corresponding to 8 sensors placed on the finger, are selected as test samples **(Fig. 4(a))**. There are two outputs, VUE and VBE, one is the vertical output voltage from the upper electrode and the bottom electrode (VUE), and the other is the horizontal output voltage from the bottom electrode and the reference electrode (V_{BE}) (**Fig. 4(b)**).

These two channels represent the press point pressure level and distance to the reference electrode separately. The resistance of the hydrogel is relative to the conductive distance; therefore, sensors with different locations can be identified. From **Fig. 4(a)**, we can find that although the array is compressed from 8 channels to 2, it can be noticed that contact-point reconstruction attains 95.33% accuracy, which means the reduction of channel numbers doesn't sacrifice the characteristics of different sensing points.

In **Fig. 5,** the object recognition capability of the palm E-skin with 40 sensing pixels is demonstrated. Based on the discussion in **Fig. 4**, it has been validated that simplifying channels through in-sensor computing does not sacrifice the characteristics of each sensor. Therefore, compared to the data volume required by traditional methods that use 40 channels, the current computational E-Skin reduces outputs to 2 channels, achieving a 95% reduction in readout dimensionality and a corresponding decrease in data volume and bandwidth (**Fig. 5(a)**). Twenty-nine everyday objects are selected to test their object discrimination capability using the 2 consolidated output channels, with the VUE indicating the contact area and contact force, and the VBE showing the contact position and shape (**Fig. 5(b)**). A high accuracy of 99.25% is successfully achieved. The differences in output curves are the cumulative result of factors such as the material, weight, hardness, and roughness of the object. The results highlight the computational E-Skin's capability for low-latency, low-power operation in the most straightforward manner for future cognitive robots.

CONCLUSION

E-Skin increasingly serves as a core platform for wearable and robotic tactile sensing, and its capabilities directly determine the ceiling of human–computer and human–robot interaction. The realization of human-augmented E-Skin perception—where subtle variations in material hardness, roughness, and composition are converted into rich electrical signatures—marks a substantive step toward contact-aware, perception-rich robotic touch. The present E-Skin combines self-powered operation, fast response, stretchability, flexibility, and multimodal signal integration. Single-pixel fingertips classify hardness and roughness with 95.0% and 92.8% accuracy and distinguish 20 visually similar materials with

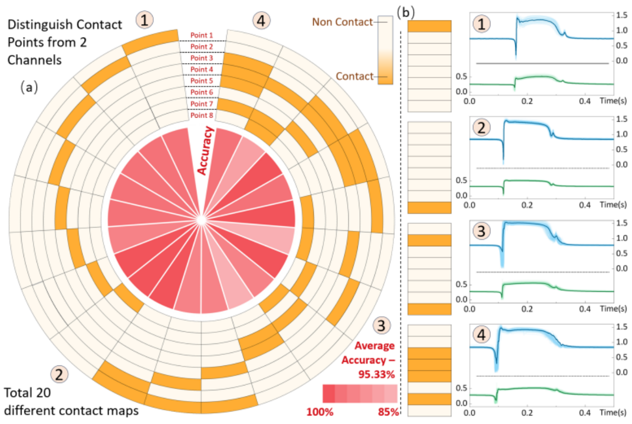

Figure 4: Location Decouple from 2 Channels: (a) 20 classes of contact points and accuracy and (b) The outputs of 4 classes from them

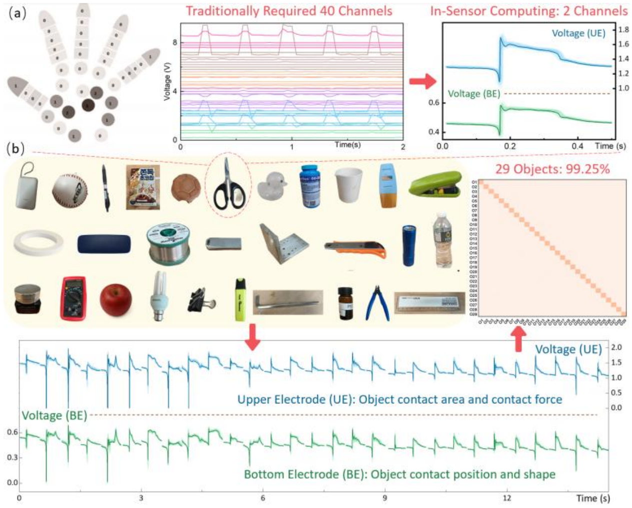

Figure 5: (a) Significantly reduce data volume and channels; (b) 29 Objects discrimination, output curves, and accuracy

98.83% accuracy, achieving human-augmented perceptual resolution while remaining compatible with soft, conformal form factors.

At the palm level, the large-area E-Skin leverages a device-intrinsic in-sensor computing architecture that realizes geometry-defined channel compression while preserving salient per-pixel information through accurate contact-point reconstruction. Under self-powered operation, the compressed two-channel readout identifies 29 daily objects with 99.25% accuracy, illustrating robust recognition across diverse tactile scenarios. The soft, biocompatible platform relies on simple, scalable fabrication routes and low-cost materials, and the underlying N-to-2 mapping principle generalizes to other array sizes and modalities. By shifting part of the computational load from electronics into the material itself, it alleviates data-bandwidth and processing bottlenecks that traditionally limit the performance of high-density tactile arrays. Overall, this geometry-programmed, self-powered computational E-Skin establishes a concrete pathway toward large-area, low-bandwidth, ultra-low-power tactile interfaces for future robotic systems.

ACKNOWLEDGEMENTS

This work is supported by RIE 2025– Industry Alignment Fund– Industry Collaboration Projects (IAF-ICP) (Grant I2301E0027) and Research Platform for Biomedical and Health Technology (RP-BTH-Prof. LEE Chengkuo) in NUS (Suzhou) Research Institute.

REFERENCES

[1] T. Jin *et al.*, "Triboelectric nanogenerator sensors for soft robotics aiming at digital twin applications," *Nat. Commun.*, vol. 11, no. 1, p. 5381, Oct. 2020

[2] T. Wu, H. Deng, Z. Sun, X. Zhang, C. Lee, and X. Zhang, "Intelligent soft robotic fingers with multi-modality perception ability," *iScience*, vol. 26, no. 8, p. 107249, 2023

[3] Q. Shi, Z. Sun, X. Le, J. Xie, and C. Lee, "Soft Robotic Perception System with Ultrasonic Auto-Positioning and Multimodal Sensory Intelligence," *ACS Nano*, vol. 17, no. 5, pp. 4985–4998, Mar. 2023

[4] X. Zhao, Z. Sun, and C. Lee, "Augmented Tactile Perception of Robotic Fingers Enabled by AI-Enhanced Triboelectric Multimodal Sensors," *Adv. Funct. Mater.*, vol. 34, no. 49, p. 2409558, Dec. 2024

[5] Y. Xu *et al.*, "Bionic e-skin with precise multi-directional droplet sliding sensing for enhanced robotic perception," *Nat. Commun.*, vol. 15, no. 1, p. 6022, Jul. 2024

[6] H. Wang, H. Wu, D. Hasan, T. He, Q. Shi, and C. Lee, "Self-Powered Dual-Mode Amenity Sensor Based on the Water–Air Triboelectric Nanogenerator," *ACS Nano*, vol. 11, no. 10, pp. 10337–10346, Oct. 2017

[7] Z. Shen *et al.*, "A Review of Non-Invasive Continuous Blood Pressure Measurement: From Flexible Sensing to Intelligent Modeling," *AI Sensors*, vol. 1, no. 2, p. 8, Nov. 2025

[8] J. Chen *et al.*, "Innovations in Multidimensional Force Sensors for Accurate Tactile Perception and Embodied Intelligence," *AI Sensors*, vol. 1, no. 2, p. 7, Sep. 2025

[9] C. Sun *et al.*, "Self-powered multifunctional monitoring system using hybrid integrated triboelectric nanogenerators and piezoelectric microsensors," *Nano Energy*, vol. 58, no. November 2018, pp. 612–623, Apr. 2019

[10] H. Wang *et al.*, "Triboelectric liquid volume sensor for self-powered lab-on-chip applications," *Nano Energy*, vol. 23, pp. 80–88, May 2016

[11] M. Gao, T. Sun, Y. Li, Z. Zhang, C. Lee, and J. Choi, "AI-Enabled Metal-Polymer Plain Bearing Based on the Triboelectric Principle," *Adv. Funct. Mater.*, vol. 33, no. 48, p. 2304070, Nov. 2023

[12] Z. Zhang *et al.*, "Artificial intelligence of toilet (AI-Toilet) for an integrated health monitoring system (IHMS) using smart triboelectric pressure sensors and image sensor," *Nano Energy*, vol. 90, no. PA, p. 106517, Dec. 2021

[13] H. Wang, J. Wang, T. He, Z. Li, and C. Lee, "Direct muscle stimulation using diode-amplified triboelectric nanogenerators (TENGs)," *Nano Energy*, vol. 63, no. June, p. 103844, Sep. 2019

[14] X. Guo, Z. Sun, Y. Zhu, and C. Lee, "Zero-Biased Bionic Fingertip E-Skin with Multimodal Tactile Perception and Artificial Intelligence for Augmented Touch Awareness," *Adv. Mater.*, vol. 36, no. 39, p. 2406778, Sep. 2024

[15] X. Zheng *et al.*, "A Bionic Textile Sensory System for Humanoid Robots Capable of Intelligent Texture Recognition," *Adv. Mater.*, vol. 37, no. 32, p. 2417729, Aug. 2025

[16] M. Zhu, T. He, and C. Lee, "Technologies toward next generation human machine interfaces: From machine learning enhanced tactile sensing to neuromorphic sensory systems," *Appl. Phys. Rev.*, vol. 7, no. 3, Sep. 2020

[17] Z. Bai, Y. Xu, C. Lee, and J. Guo, "Autonomously Adhesive, Stretchable, and Transparent Solid-State Polyionic Triboelectric Patch for Wearable Power Source and Tactile Sensor," *Adv. Funct. Mater.*, vol. 31, no. 37, p. 2104365, Sep. 2021

[18] Y. Liu *et al.*, "Triboelectric tactile sensor for pressure and temperature sensing in high-temperature applications," *Nat. Commun.*, vol. 16, no. 1, p. 383, Jan. 2025

[19] Z. Zhang, L. Wang, and C. Lee, "Recent Advances in Artificial Intelligence Sensors," *Adv. Sens. Res.*, vol. 2, no. 8, Aug. 2023

[20] L. Wang, X. Guo, Z. Zhang, and C. Lee, "Metaverse-Enabled Yoga Coach Avatar Using AI-Enhanced Multimodal Insole Sensing System," *Adv. Funct. Mater.*, p. 2519562, Oct. 2025

[21] L. Liu *et al.*, "Innovative smart gloves with Phalanges-based triboelectric sensors as a dexterous teaching interface for Embodied Artificial Intelligence," *Nano Energy*, vol. 133, no. November 2024, p. 110491, 2025

[22] Z. Yan *et al.*, "Flexible High-Resolution Triboelectric Sensor Array Based on Patterned Laser-Induced Graphene for Self-Powered Real-Time Tactile Sensing," *Adv. Funct. Mater.*, vol. 31, no. 23, p. 2100709, Jun. 2021

CONTACT

*C. Lee; elelc@nus.edu.sg